

Using concatenated algebraic geometry codes in channel polarization

Abdulla Eid and Iwan Duursma*

September 10, 2018

Abstract

Polar codes were introduced by Arikan [1] in 2008 and are the first family of error-correcting codes achieving the symmetric capacity of an arbitrary binary-input discrete memoryless channel under low complexity encoding and using an efficient successive cancellation decoding strategy. Recently, non-binary polar codes have been studied, in which one can use different algebraic geometry codes to achieve better error decoding probability. In this paper, we study the performance of binary polar codes that are obtained from non-binary algebraic geometry codes using concatenation. For binary polar codes (i.e. binary kernels) of a given length n , we compare numerically the use of short algebraic geometry codes over large fields versus long algebraic geometry codes over small fields. We find that for each n there is an optimal choice. For binary kernels of size up to $n \leq 1,800$ a concatenated Reed-Solomon code outperforms other choices. For larger kernel sizes concatenated Hermitian codes or Suzuki codes will do better.

1 Introduction to Channel Polarization

Polar codes were introduced by Arikan [1] in 2008 and are the first family of error-correcting codes achieving the symmetric capacity of an arbitrary binary-input discrete memoryless channel under low complexity encoding

*eid1@illinois.edu, duursma@math.illinois.edu

and using an efficient successive cancellation decoding strategy. We introduce now the polar codes and the channel polarization phenomenon for a q -ary input symmetric discrete memoryless channel W with input alphabet \mathcal{X} and output alphabet \mathcal{Y} . We start first with some notations from [10],[13],[14].

Notation 1. Let u_0^{N-1} be the vector $u = (u_0, \dots, u_{N-1}) \in \mathcal{X}^N$ ($N \in \mathbb{N}_{>0}$). For each $0 \leq i < j \leq N-1$, we denote by u_i^j the subvector $(u_i, \dots, u_j) \in \mathcal{X}^{j-i+1}$ of u . Moreover, if $\mathcal{F} := \{f_0 < \dots < f_t\} \subseteq \{0, 1, \dots, N-1\}$ is a set of indices, then we denote by $u_{\mathcal{F}}$ the subvector $(u_{f_0}, \dots, u_{f_t}) \in \mathcal{X}^{t+1}$ of u .

Let $W : \mathcal{X} \rightarrow \mathcal{Y}$ be a q -ary input discrete memoryless channel with a uniform distribution on the input alphabet \mathcal{X} . Let $\ell \geq 2$ be a positive integer and $g : \mathcal{X}^\ell \rightarrow \mathcal{X}^\ell$ be an \mathbb{F}_q -isomorphism linear map, which is called the *kernel* map. Let $G \in \text{Mat}(\ell, \ell, \mathcal{X})$ be the matrix representing the map g and $G^{\otimes n}$ be the n th Kronecker product of G of size $\ell^n \times \ell^n$.

Definition 2. For $i \geq 1$, the *subchannel* $W^{(i)} : \mathcal{X} \rightarrow \mathcal{Y}^{\ell^n} \times \mathcal{X}^i$ is defined as the channel on input u_i , output $(y_0^{\ell^n-1}, u_0^{i-1})$, and probability distribution

$$W^{(i)}(y_0^{\ell^n-1}, u_0^{i-1} | u_i) := \frac{1}{q^{\ell^n}} \sum_{u_{i+1}^{\ell^n-1} \in \mathcal{X}^{\ell^n-i+1}} W(y_0^{\ell^n-1} | u_0^{\ell^n-1} G^{\otimes n}).$$

Let $\{B_i\}_{i \in \mathbb{N}_{>0}}$ be a sequence of independent and identically distributed random variables defined over some probability space such that $B_i = k$ with probability $1/\ell$, for each $k = 1, 2, \dots, \ell$. Define the random process $\{W_n | n \in \mathbb{N}\}$ recursively by

$$\begin{aligned} W_0 &:= W, \\ W_{n+1} &:= W_n^{(B_{n+1})}. \end{aligned}$$

Recall that the symmetric capacity and the Bhattacharyya parameter of a q -ary input discrete memoryless channel $W : \mathcal{X} \rightarrow \mathcal{Y}$ is defined as

$$I(W) := \frac{1}{q} \sum_{x \in \mathcal{X}} \sum_{y \in \mathcal{Y}} W(y | x) \log_q \frac{W(y | x)}{\frac{1}{q} \sum_{x' \in \mathcal{X}} W(y | x')}.$$

and

$$Z(W) := \frac{1}{q(q-1)} \sum_{\substack{x, x' \in \mathcal{X} \\ x' \neq x}} \sum_{y \in \mathcal{Y}} \sqrt{W(y | x)W(y | x')}.$$

Set $I_n := I(W_n)$ and $Z_n := Z(W_n)$. Then,

Lemma 3. [17, Lemma 2] [13, Lemma 9] *There exists a random variable I_∞ such that $I_n \rightarrow I_\infty$ almost surely as $n \rightarrow \infty$.*

Using the lemma above, the channel polarization occurs if the probability that $I_\infty \in \{0, 1\}$ is one. The term "polarization" refers to the fact that the subchannels *polarize* to noiseless channels or pure-noisy channels [1].

Definition 4. A *polar code* is a code with kernel G such that in the construction above, $Pr(I_\infty \in \{0, 1\}) = 1$ and

$$I_\infty = \begin{cases} 1, & \text{w.p. } I(W), \\ 0, & \text{w.p. } 1 - I(W). \end{cases} \quad (1)$$

From the definition above, we see that a repeated application of the matrix G polarizes the underlying channel, i.e., the resulting subchannels $W^{(i)}$ ($i \in \{1, \dots, \ell^n\}$) tend toward either noiseless channels or pure-noisy channels. Moreover, Condition (1) guarantees that the fraction of the noiseless channels to all channels approaches $I(W)$, i.e., polar codes are capacity achieving. That suggests using the noiseless channels for transmitting the information symbols while transmitting no information over the pure-noisy channels, which are called the frozen symbols [1].

The polar codes introduced by Arikan [1] in 2008 use the 2×2 matrix

$$G_2 = \begin{pmatrix} 1 & 0 \\ 1 & 1 \end{pmatrix}.$$

Thereafter, Urbanke, Korada, and Sasöglu generalized Arikan's construction for BSCs. They showed that any $\ell \times \ell$ matrix G , none of whose column permutations is an upper triangular matrix, polarizes the channel. Mori and Tanaka [13] generalized the idea further to q -ary input S-DMC.

Polar codes have been found to be useful for many applications. They can be used to construct a lossy and lossyless source channel that achieve the rate-distortion trade-off with low encoding and decoding complexity, i.e., they have an optimal performance in that setting [8]. Polar codes can also be used for deterministic broadcast channels [5], to achieve the secrecy capacity of wiretap channels [12], and in ubiquitous computing and sensor network applications [11].

We conclude this section by giving sufficient condition for an non-identity $\ell \times \ell$ matrix G to polarize the q -ary input S-DMC W .

Theorem 5. [10, Theorem 4],[13, Theorem 13] (*q is a prime integer*) Given a *q*-ary input symmetric discrete memoryless channel *W*, any $\ell \times \ell$ matrix *G* none of whose column permutations is an upper triangular polarizes the channel.

Remark 6. Let *G* be an $\ell \times \ell$ matrix and *U* be an $\ell \times \ell$ upper triangular matrix. Then, the channels $W^{(i)}$ have the same statistical properties under *G* and *GU*, i.e., *G* and *GU* are equivalent in the sense of Definition 4 in [15]. Moreover, column permutations also do not change the statistical properties of $W^{(i)}$. Therefore, using an *LUP* decomposition we may assume that *G* itself is a lower triangular matrix.

Theorem 7. [15, Theorem 11] (*q is a prime power*) Let \mathbb{F}_q be a non-prime finite field of characteristic *p*. Given a *q*-ary input symmetric discrete memoryless channel *W*, then an $\ell \times \ell$ lower triangular matrix *G* polarizes the channel *W* if and only if $\mathbb{F}_q = \mathbb{F}_p(G)$, where $\mathbb{F}_p(G)$ is the field extension of \mathbb{F}_p generated by the entries of *G*.

2 The Performance of Polar Codes and the Rate of Polarization

In this section we explain the asymptotic error probability and how it depends on the exponent of the kernel, a quantity that plays an important role in determining the performance of polar codes.

2.1 The Error Probability

The performance of the polar code is determined based on the asymptotic error probability. In Arikan's construction of a binary polar code [2] using the matrix G_2 , the asymptotic error probability of the polar code using the successive cancellation decoding is

$$P_{\text{err}} = \begin{cases} o\left(2^{-N^\beta}\right), & \beta < \frac{1}{2}, \\ \omega\left(2^{-N^\beta}\right), & \beta \geq \frac{1}{2}. \end{cases} \quad (2)$$

The error probability P_{err} above¹ is independent of the rate R of the polar code. Mori and Tanaka [19] extended the formula above to one that is rate dependent. Moreover, the threshold $1/2$ depends only on the matrix G_2 and not on the underlying channel W .

Now for any $\ell \times \ell$ matrix G that polarizes the q -ary input S-DMC W , the asymptotic error probability of the polar code is given by

$$P_{\text{err}} = \begin{cases} o\left(2^{-N^\beta}\right), & \beta < E(G), \\ \omega\left(2^{-N^\beta}\right), & \beta \geq E(G) \end{cases} \quad (3)$$

for some well-defined constant $E(G) \in [0, 1)$ depending only on the matrix G and not on the underlying channel W . The quantity $E(G)$ is called the *exponent* of the matrix G . It measures the performance of the polar code under successive cancellation decoding ([10, Section IV] for $q = 2$ and [13, Theorem 9] for any $q > 2$).

Remark 8. As in [13, Theorem 19], Equation (3) can be read as follows. For any kernel which polarizes the underlying channel it holds

$$\lim_{n \rightarrow \infty} Pr(Z_n < 2^{\ell - n^\beta}) = I(W)$$

for $\beta < E(G)$ and

$$\lim_{n \rightarrow \infty} Pr(Z_n < 2^{\ell - n^\beta}) = 0$$

for $\beta > E(G)$.

2.2 The Formula of the Exponent

As mentioned in the previous subsection, the exponent of the matrix G plays an important role in determining the performance of the polar codes. In [10],[14], the authors gave an algebraic description of the exponent in terms of the partial distances of the matrix G .

Definition 9. Given an $\ell \times \ell$ matrix $G = (g_1, \dots, g_\ell)^T \in \text{Mat}(\ell, \ell, \mathbb{F}_q)$, the *partial distances* D_i ($i = 1, 2, \dots, \ell$) are defined by

$$\begin{aligned} D_\ell &:= \text{wt}(g_\ell) = d(g_\ell, 0), \\ D_i &:= d(g_i, \langle g_{i+1}, \dots, g_\ell \rangle), \end{aligned}$$

¹The parameter β is an arbitrary real number, if $\beta < 1/2$, then there exists a polar code that satisfies $P_{\text{err}} = o\left(2^{-N^\beta}\right)$

where $d(g_i, \langle g_{i+1}, \dots, g_\ell \rangle)$ is the distance from the codeword g_i to the code generated by the codewords g_{i+1}, \dots, g_ℓ . The partial distances $\{D_i\}_{i=1}^\ell$ of a matrix G will be called the *profile* of G .

Theorem 10. [10, Theorem 14],[14, Theorem 1] *Let W be a q -ary input symmetric discrete memoryless channel and G be an $\ell \times \ell$ matrix that polarizes the channel W with profile $\{D_i\}_{i=1}^\ell$. Then, the exponent of G is given by*

$$E(G) = \frac{1}{\ell} \sum_{i=1}^{\ell} \log_{\ell} D_i. \quad (4)$$

For q -ary codes, Mori and Tanaka [14] suggested using algebraic geometry codes in order to get larger exponents. The motivation behind this idea is the Reed-Solomon code which gives large exponents. In particular, algebraic geometry codes have in general large minimum distance and often they have a nested structure similar to the Reed-Solomon code which makes them suitable for channel polarization.

2.3 Concatenation

In this section we introduce the *concatenation* of codes which is illustrated in the following theorem.

Theorem 11. [16, Theorem 6.3.1] *Let C_1 be a (N, K, D) -linear code over \mathbb{F}_{q^m} and C_2 be a (n, m, d) -linear code over \mathbb{F}_q . Then, there exists a (nN, mK, dD) -linear code C over \mathbb{F}_q .*

The code C_1 in Theorem 11 is called the *outer code*, the code C_2 is called the *inner code*, and the code C is called the *concatenated code*. In the following, we will use the descent code $(\mathbb{F}_q)^m$ which is a $(m, m, 1)$ -linear code as an inner code and all field extensions \mathbb{F}_q are of characteristic 2. Therefore, given a (N, K, D) -linear code over \mathbb{F}_{2^m} , Theorem 11 yields a binary (mN, mK, D) -linear code.

Let $G \in \text{Mat}(L, L, \mathbb{F}_q)$ be a generating matrix for a code over \mathbb{F}_q and let (D_1, \dots, D_L) be its profile. Recall that the exponent of G is given by

$$E(G) := \frac{1}{L} \sum_{i=1}^L \log_L D_i = \frac{1}{L \log_2 L} \sum_{i=1}^L \log_2 D_i.$$

Applying the inner code $(m, m, 1)$ to the matrix G will replace each symbol in G with m binary symbols and each row will be redundant m times. Therefore, the new concatenated matrix, denoted by G_2 , will be of size $mL \times mL$, and will have at least the following profile

$$\underbrace{D_1, \dots, D_1}_{m\text{-times}}, \underbrace{D_2, \dots, D_2}_{m\text{-times}}, \dots, \underbrace{D_L, \dots, D_L}_{m\text{-times}}.$$

Then, the exponent of the binary matrix G_2 satisfies the inequality

$$\begin{aligned} E(G_2) &:= \frac{1}{mL \log_2(mL)} \cdot m \cdot \sum_{i=1}^L \log_2 D_i \\ &\geq \frac{1}{L \log_2(mL)} \cdot L \cdot \log_2 L \cdot E(G) \\ &\geq \frac{\log_2 L}{\log_2(mL)} \cdot E(G). \end{aligned}$$

2.4 Our Results

Mori and Tanaka [14] evaluated the performance of polar codes using kernels constructed from the generating matrices of the Reed-Solomon and Hermitian codes over a q -ary field. They have found that numerically Hermitian codes give larger exponents than Reed-Solomon codes. That suggests using different algebraic geometry codes as they have large minimum distance and often have the same nested structure as Reed-Solomon codes. We continue in this direction by using algebraic geometry codes to study the behavior of the exponent. In Section 3 we show for a subclass of algebraic geometry codes, that $E(G_L) \rightarrow 1$ as the number of affine rational points $L \rightarrow \infty$.

In Section 4 we will apply the concatenation of codes to construct binary codes from q -ary codes. As the algebraic geometry codes are defined over different field extensions of \mathbb{F}_2 . This helps us to study the performance of different algebraic geometry codes defined over a common field which is the binary field \mathbb{F}_2 . We will study numerically whether to use larger field extensions or curves with many rational points to get a larger exponent. In other words, it is the study of how to approach ∞ in the most efficient way using either concatenation or geometry. In the first case (concatenation) we would need codes defined over large fields and in the second case (geometry) we would need curves with many rational points defined over small fields.

In Section 5 we compare numerically how the Reed-Solomon, Hermitian, and Suzuki codes behave in the settings above for a given binary block size. It turns out that each code will give the maximum exponent for some range of the binary block size, and that more geometry is preferable as the block size increases. We also compare their performance as error-correcting codes.

3 The Algebraic Geometry Codes in Channel Polarization

In this section we recall first the construction of the algebraic geometry codes. We give three examples of algebraic geometry codes, the Reed-Solomon code, the Hermitian code, and the Suzuki code. Moreover, we will show in this section that for a subclass of algebraic geometry codes with block length L and generating matrix G_L , we have $E(G_L) \rightarrow 1$ as $L \rightarrow \infty$.

3.1 Algebraic Geometry Codes as Kernels for Channel Polarization

Let X/\mathbb{F}_q be a curve (smooth, irreducible, and projective) of genus g over \mathbb{F}_q with global function field $F := \mathbb{F}_q(X)$. Let $X(\mathbb{F}_q)$ be the set of all \mathbb{F}_q -rational points on X with cardinality $N(F)$. Let $1 \leq n < N(F)$ and choose n distinct rational places $P_1, \dots, P_n \in X(\mathbb{F}_q)$. Set $D := P_1 + \dots + P_n$ and let $G' := \sum_{i=1}^s n_i Q_i - \sum_{j=1}^t m_j Q'_j \in \text{Div}(X)$ ($n_i, m_j \in \mathbb{N}$) be a divisor of X such that $\text{Supp}(D) \cap \text{Supp}(G') = \emptyset$. Define the Riemann-Roch space $\mathcal{L}(G')$ to be the \mathbb{F}_q -vector space of all rational functions $f \in F$ which are having only poles at Q_i of order less than or equal to n_i and zeros at Q'_i of order greater than or equal to m_j , i.e.,

$$\mathcal{L}(G') := \{f \in F \mid (f) + G' \geq 0\} \cup \{0\}$$

Then, the algebraic geometry code is defined as

$$C_{\mathcal{L}}(D, G') := \{(f(P_1), \dots, f(P_n)) \in \mathbb{F}_q^n \mid f \in \mathcal{L}(G')\}.$$

The code $C_{\mathcal{L}}(D, G')$ is a (n, k, d) -linear code over \mathbb{F}_q , where $k := \ell(G') - \ell(G' - D)$ and $d \geq d^* := n - \deg(G')$. Moreover, assume $n > \deg(G')$ and let

$\{f_1, \dots, f_k\}$ be a basis for $\mathcal{L}(G')$ over \mathbb{F}_q . Then, $C_{\mathcal{L}}(D, G')$ has the following generator matrix

$$G := (f_i(P_j))_{\substack{i=1, \dots, k \\ j=1, \dots, n}}.$$

Example 12. (Reed-Solomon Code) Let $F := \mathbb{F}_q(x)$ be the rational function field that corresponds to the projective line $\mathbb{P}^1(\mathbb{F}_q)$. Let $P_1, \dots, P_q \in \mathbb{P}_F$ be the affine rational places of F . Set $G' := dP_{\infty}$ ($d < q$). The set $\{1, x, x^2, \dots, x^d\}$ is a basis for $\mathcal{L}(dP_{\infty})$ over \mathbb{F}_q . Then, the Reed-Solomon code of length q is the algebraic geometry code $C_{\mathcal{L}}(P_1 + \dots + P_q, dP_{\infty})$.

Example 13. (Hermitian Code) Let $F_{\mathbb{H}} := \mathbb{F}_q(x, y)$ be the Hermitian function field of genus $g_{\mathbb{H}} = q_0(q_0 - 1)/2$ over \mathbb{F}_q ($q := q_0^2$ and q_0 is a prime power) defined by the equation $y^{q_0} + y = x^{q_0+1}$. Let $P_1, \dots, P_{q_0^3} \in \mathbb{P}_{F_{\mathbb{H}}}$ be the affine \mathbb{F}_q -rational places of $F_{\mathbb{H}}$. Set $G' := dP_{\infty}$ ($d < q_0^3$). The set $\{x^i y^j \mid i \geq 0, i q_0 + j(q_0 + 1) \leq d\}$ is a generating set for $\mathcal{L}(dP_{\infty})$ over \mathbb{F}_q [18, Lemma 6.4.4]. Then, the Hermitian code of length q_0^3 is the algebraic geometry code $C_{\mathcal{L}}(P_1 + \dots + P_{q_0^3}, dP_{\infty})$.

Example 14. (Suzuki Code) Let $F_{\mathbb{S}} := \mathbb{F}_q(x, y)$ be the Suzuki function field of genus $g_{\mathbb{S}} = q_0(q - 1)$ over \mathbb{F}_q ($q := 2q_0^2$, $q_0 = 2^m$, and $m \in \mathbb{N}$) defined by the equation $y^q - y = x^{q_0}(x^q - x)$. Let $P_1, \dots, P_{q^2} \in \mathbb{P}_{F_{\mathbb{S}}}$ be the affine \mathbb{F}_q -rational places of $F_{\mathbb{S}}$. Set $G' := dP_{\infty}$ ($d < q^2$). The set $\{x^a y^b z^c w^{d'} \mid a, b, c, d' \geq 0, aq + b(q + q_0) + c(q + 2q_0) + d'(q + 2q_0 + 1) \leq d\}$ is a generating set for $\mathcal{L}(dP_{\infty})$ over \mathbb{F}_q [6], where $z := x^{2q_0+1} - y^{2q_0}$ and $w := xy^{2q_0} - z^{2q_0}$. Then, the Suzuki code of length q^2 is the algebraic geometry code $C_{\mathcal{L}}(P_1 + \dots + P_{q^2}, dP_{\infty})$.

3.2 The kernel $E(G)$ for Algebraic Geometry Codes

In this section we use Stirling's formula to show that $E(G_L) \rightarrow 1$ as $L \rightarrow \infty$, where G_L is the generating matrix of an algebraic geometry code of block length L . First we state the Oesterlé bound (see [7, Theorem 8, page 130]) which gives a lower bound to the genus g of a curve X/\mathbb{F}_q with L affine rational points. Let ℓ be the unique integer such that $\sqrt{q}^{\ell} < L \leq \sqrt{q}^{\ell+1}$, i.e.,

$$\ell = \left\lceil \frac{\log_2 L}{\log_2 \sqrt{q}} - 1 \right\rceil. \quad (5)$$

We find

$$u := \frac{\sqrt{q}^{\ell+1} - L}{L\sqrt{q} - \sqrt{q}^{\ell}} \in [0, 1). \quad (6)$$

Next, we find $\theta \in [\pi/(\ell + 1), \pi/\ell)$ such that

$$\cos\left(\frac{\ell + 1}{2}\theta\right) + u \cos\left(\frac{\ell - 1}{2}\theta\right) = 0. \quad (7)$$

Then, the Oesterlé bound is the lower bound

$$g \geq \frac{(L - 1)\sqrt{q} \cos \theta + q - L}{q + 1 - 2\sqrt{q} \cos \theta}. \quad (8)$$

Note that for some small L , this bound can be achieved by maximal curves over \mathbb{F}_{q^2} or for large L by towers of function fields. We will study the case where $g := ((L - 1)\sqrt{q} \cos \theta + q - L) / (q + 1 - 2\sqrt{q} \cos \theta)$.

Remark 15. If L is small relative to the field size q (e.g., $L < \sqrt{q}$), then the right hand side of the Inequality (8) is negative. In that case we take $g = 0$ as the code can be achieved by Reed-Solomon codes as in Example 12.

Now we prove the result of this section. Here we will study only the subclass of algebraic geometry codes over \mathbb{F}_q with a matrix $G_L \in \text{Mat}(L, L, \mathbb{F}_q)$ that has profile²

$$D_i := \begin{cases} L - g + 1 - i, & i = 1, 2, \dots, L - g, \\ 1, & i = L - g + 1, \dots, L. \end{cases} \quad (9)$$

Therefore,

$$E(G_L) = \frac{\log_q((L - g)!)}{L \log_q L}. \quad (10)$$

Proposition 16. *For the class of algebraic geometry codes over a fixed field \mathbb{F}_q of length L and matrix G_L with profile $D_i = \max(L - g + 1 - i, 1)$ ($i = 1, \dots, L$), we have*

$$E(G_L) \rightarrow 1 \quad \text{as} \quad L \rightarrow \infty.$$

Proof. Recall Stirling's formula [3]

$$\lim_{n \rightarrow \infty} \frac{n!}{\sqrt{2\pi n} \left(\frac{n}{e}\right)^n} = 1$$

²The least possible profile for a nested structure AG code using the point at infinity

which is equivalent to

$$n! \simeq \sqrt{2\pi n} \left(\frac{n}{e}\right)^n.$$

Therefore, we get the estimate

$$\log(n!) = n \log n - n + O(\log n), \quad \text{where } O(\log n) \simeq \frac{1}{2} \log(2\pi n).$$

Now we have

$$\begin{aligned} E(G_L) &= \frac{\log_q((L-g)!) }{L \log_q L} \\ &= \frac{1}{L \log L} [(L-g) \log(L-g) - (L-g) + O(\log(L-g))] \\ &= \frac{L-g}{L} \cdot \frac{\log(L-g)}{\log(L)} - \frac{L-g}{L \log(L)} + \frac{1}{2} \cdot \frac{\log(2\pi(L-g))}{L \log(L)}. \end{aligned}$$

Recall that

$$g = \frac{(L-1)\sqrt{q} \cos \theta + q - L}{q+1-2\sqrt{q} \cos \theta} = \frac{L(\sqrt{q} \cos \theta - 1) - \sqrt{q} \cos \theta + q}{q+1-2\sqrt{q} \cos \theta}.$$

Then,

$$\begin{aligned} L-g &= L \left[1 - \frac{(\sqrt{q} \cos \theta - 1) - \frac{\sqrt{q} \cos \theta}{L} + \frac{q}{L}}{q+1-2\sqrt{q} \cos \theta} \right] \\ &\simeq L \left[1 - \frac{\sqrt{q} \cos \theta - 1}{q+1-2\sqrt{q} \cos \theta} \right] \simeq L \left[\frac{q+2-3\sqrt{q} \cos \theta}{q+1-2\sqrt{q} \cos \theta} \right] \\ &\simeq a(q)L, \end{aligned}$$

for some constant $a(q)$ close to 1 for large q . Therefore, we have that

$$\begin{aligned} \frac{L-g}{L \log(L)} &\simeq \frac{a(q)}{\log(L)} \rightarrow 0 && \text{as } L \rightarrow \infty, \\ \frac{\log(2\pi(L-g))}{L \log(L)} &\simeq \frac{\log(2\pi a(q)L)}{L \log(L)} \rightarrow 0 && \text{as } L \rightarrow \infty, \\ \frac{L-g}{L} \cdot \frac{\log(L-g)}{\log(L)} &\simeq \frac{a(q)L}{L} \cdot \frac{\log(a(q)L)}{\log(L)} \rightarrow a(q) \rightarrow 1 && \text{as } L \rightarrow \infty. \end{aligned}$$

Therefore,

$$E(G_L) \simeq \underbrace{\frac{L-g \log(L-g)}{L \log(L)}}_{\rightarrow 1} - \underbrace{\frac{L-g}{L \log(L)}}_{\rightarrow 0} + \frac{1}{2} \underbrace{\frac{\log(2\pi(L-g))}{L \log(L)}}_{\rightarrow 0}.$$

$\rightarrow 1.$

as $L \rightarrow \infty$

□

4 Fixing the Parameters

We have seen in the previous section that asymptotically $E(G_L) \rightarrow 1$ as $L \rightarrow \infty$. In this section we would like to study numerically³ the asymptotic behavior of different algebraic geometry codes. In order to compare their performance, we need these codes to be defined over a common field which is the binary field \mathbb{F}_2 . For that, we use the concept of concatenation that was first introduced by Forney [4] as a technique to obtain new codes over the binary field from codes over a field extension of \mathbb{F}_2 , see Section 2.3.

We keep the same assumption about G as in Section 3, i.e., G is the generating matrix of an algebraic geometry code constructed using an algebraic curve of genus g with L affine rational points and profile $D_i = \max(L - g + 1 - i, 1)$ ($i = 1, \dots, L$). As in Section 2.3, the exponent of G and G_2 are related by the inequality

$$E(G_2) \geq \frac{\log_2 L}{\log_2(mL)} \cdot E(G). \quad (11)$$

Therefore, using Proposition 16, $E(G_{L,2}) \rightarrow 1$ as $L \rightarrow \infty$.

We would like to study the asymptotic behavior of $E(G_2)$ by studying the lower bound in Inequality (11). Set

$$\begin{aligned} E_2(G) &:= \frac{\log_2 L}{\log_2(mL)} \cdot E(G) = \frac{\log_2(L)}{\log_2(mL)} \cdot \frac{1}{L \log_2(L)} \cdot \log_2((L-g)!) \\ &= \frac{1}{L \log_2(mL)} \log_2((L-g)!) \end{aligned}$$

which is a function in m (field size), L (number of affine rational points), and θ (algebraic curve) (8). We denote the binary block length after concatenation by n , i.e., $n := mL$ and we will regard $E_2(G)$ as a function on n , m , and θ .

³All the computations in this section are performed by Mathematica [9]

4.1 Fixing the Binary Block Size n

Let n be a fixed binary block size. Then, $L = L(m) = n/m$ and $\theta = \theta(m)$ can be found using (7). This means that $E_2(G)$ can be written in term of m . Numerically using Mathematica, enumerating over all positive integers m shows that $E_2(G)$ has a local maximum, e.g., see Figure 1 and Table 1 for binary block size $n = 3 \cdot 2^{20}$.

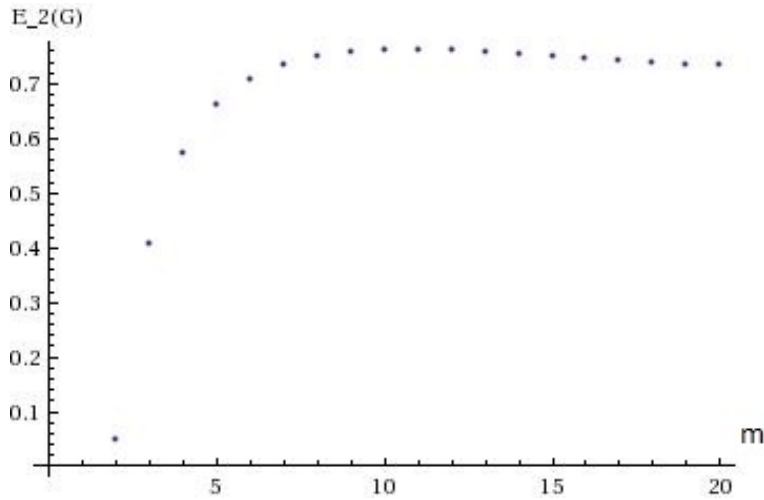


Figure 1: Fixing $n = 3 \cdot 2^{20}$ and enumerating over all m , we have a local maximum at $m=12$ which correspond to the Hermitian curve.

In Section 5, numerically as n gets larger, this local maximum corresponds first to the Reed-Solomon code for a small range of n , then it corresponds to the Hermitian code and as n gets larger, the local maximum corresponds to the Suzuki code (see Figure 5).

4.2 Fixing the Algebraic Curve θ

Let θ be fixed, i.e., the underlying algebraic curve is fixed. Then, $L = L(m)$ can be found in terms of m as follows. Find $\ell := \ell(\theta) = \lfloor \pi/\theta \rfloor$, using (7) we have

$$u = -\frac{\cos\left(\left(\frac{\ell+1}{2}\right)\theta\right)}{\cos\left(\left(\frac{\ell-1}{2}\right)\theta\right)}.$$

m	q	L	g	$E_2(G)$
2	2	1572864	$1.46820 * 10^6$	0.046959
3	8	1048576	524647.	0.406401
4	16	786432	233948.	0.573893
6	64	524288	62517.2	0.708937
8	256	393216	19901.6	0.750686
12	2^{12}	262144	2016.00	0.760667
16	2^{16}	196608	256.000	0.746789
24	2^{24}	131072	0	0.720751
32	2^{32}	98304	0	0.701524

Table 1: The values of $E_2(G)$ for $n = 3 \cdot 2^{20}$, where the maximum is at $m = 12$ which corresponds to the Hermitian curve.

Then, using (6), we get

$$L := L(m) = \frac{\sqrt{q}^{\ell+1} - u\sqrt{q}^{\ell}}{u\sqrt{q} + 1} = \frac{\sqrt{2^m}^{\ell+1} - u\sqrt{2^m}^{\ell}}{u\sqrt{2^m} + 1}.$$

Therefore, $E_2(G)$ is a function of m . In this case it turns out that $E_2(G)$ is an increasing function (see Figure 2). This means that *more concatenation gives larger exponents*.

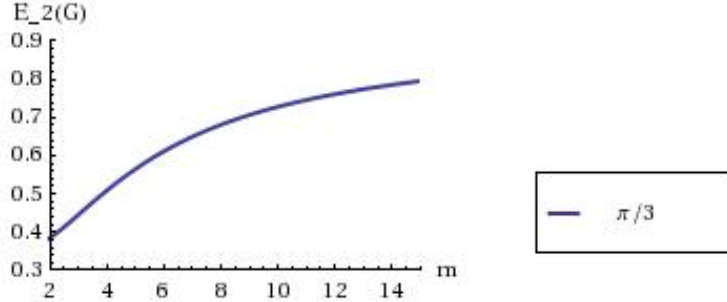


Figure 2: Fixing $\theta = \pi/3$ and enumerate over all m .

4.3 Fixing the Field Extension \mathbb{F}_{2^m}

Let m be fixed. Using (7), $\theta = \theta(L)$ and so $E_2(G)$ can be regarded as a function of L . Numerically $E_2(G)$ is an increasing function in L with limit that tends to 1 as $L \rightarrow \infty$ (see Figure 3). This means again that *more geometry gives larger exponents*.

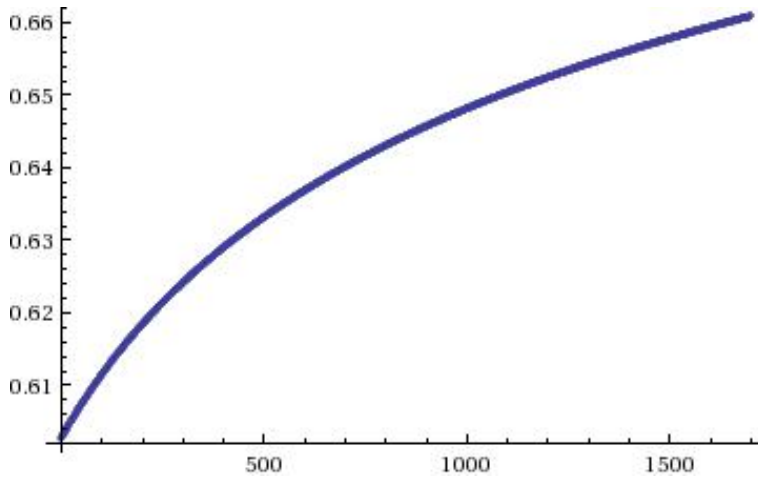


Figure 3: The exponent $E_2(G)$ if we fix $m = 8$ and enumerate on L .

Remark 17. From the two analyses above, we see that more concatenation gives larger exponents and similarly, more geometry also gives larger exponents. It is the question about the tradeoff between concatenation and geometry in how to efficiently approach the limit, i.e., $E(G) \rightarrow 1$. In Section 5, we will see that numerically for the three codes (Reed-Solomon, Hermitian, and Suzuki codes) more geometry is preferable as the block size increases.

5 A Comparison between the three Curves

In this section we will use Mathematica [9] to compare the performance of the three binary concatenated codes which are the Reed-Solomon code constructed from the projective line with $\theta = \pi/2$ (Example 12), the Hermitian code constructed from the Hermitian curve with $\theta = 2\pi/3$ (Example 13), and the Suzuki code constructed from the Suzuki curve with $\theta = 3\pi/4$ (Example 14). The two applications that will be considered in this section are the

comparison between these codes as suitable kernels for channel polarization and as suitable codes for error-correction.

5.1 A Comparison for Channel Polarization

As the rate of polarization is determined based on the exponent of the kernel, we compare numerically the three codes above as suitable kernels for channel polarization. Let n be the binary block size, we draw a graph between the values of n and the corresponding values of $E_2(G)$ for the three codes (see Figure 4). From the graph we notice that as n gets larger, the maximum

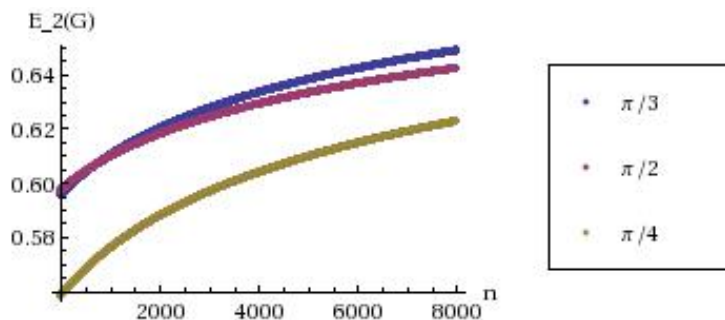


Figure 4: The exponent $E_2(G)$ using $\theta = \pi/3, \pi/4, \pi/2$ and enumerating over the binary block size n . We notice when $n = 10000$, the three curves from top to bottom will correspond to $\theta = \pi/3, \pi/2, \pi/4$. For $n \geq 400,000$, the Suzuki code will be in the top, then the Hermitian code and finally the Reed-Solomon code

$E_2(G)$ is attained first by the Reed-Solomon codes for values of $n < 1800$, after that as n gets larger, by the Hermitian codes up to $n = 399,212$ and after that by the Suzuki codes. This can be generalized to any $\theta = k\pi/\ell$, i.e., more geometry yields larger exponents as $n \rightarrow \infty$. We summarize this result in Figure 5.

5.2 A Comparison for Error-Correction

In this section we compare the performance of the three codes above as error-correcting codes with fixed binary rate. We draw a graph between the binary block size n and $(k+d)/n$, where n , k , and d are the parameters of the binary concatenated code with fixed binary rate.

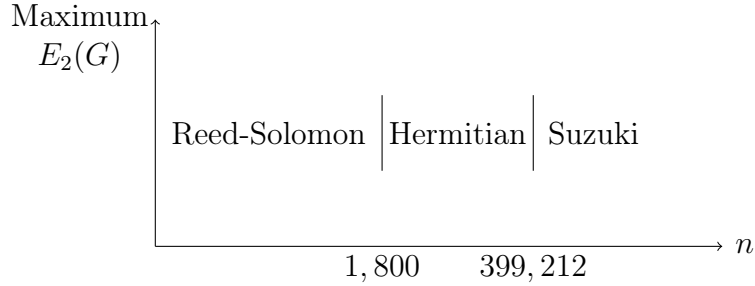


Figure 5: The maximum exponent for a given n is obtained with the indicated choice of curve.

For that, let C be an algebraic geometry code with parameters (L, K, D) over \mathbb{F}_{2^m} constructed from the algebraic curve of genus g with L affine rational points. Then, we have

$$L - g + 1 \leq K + D < L + 1 \Rightarrow \frac{L - g + 1}{L} \leq \frac{K + D}{L} < \frac{L + 1}{L}.$$

Assume $(K + D)/L = (L - g + 1)/L$ [20, Corollary 4.1.14, p. 196]. Then, the concatenated binary code has parameters (mL, mK, d') ($d' \geq D$). Therefore,

$$\frac{mK + d'}{mL} \geq \frac{mK + D}{mL} = \underbrace{\frac{(m-1)}{m}}_{\text{known}} \cdot \underbrace{\frac{K}{L}}_{\text{Rate}} + \underbrace{\frac{K + D}{mL}}_{\text{known}} = \frac{m-1}{m} \frac{K}{L} + \frac{L - g + 1}{mL}.$$

Therefore, we can draw the graph between n and $(k + d)/n$ as in Figure 6.

Figure 6 shows that as $n \rightarrow \infty$, $(k + d)/n \rightarrow R = 1/2$ and for the first few values of n , the Reed-Solomon code is the closest code to the line $y = 1/2$, then comes the Hermitian code to be the closest and as n gets larger, the Suzuki code is the code that is closest to the line $y = 1/2$, so we have once again that more geometry is preferable as the block size increases.

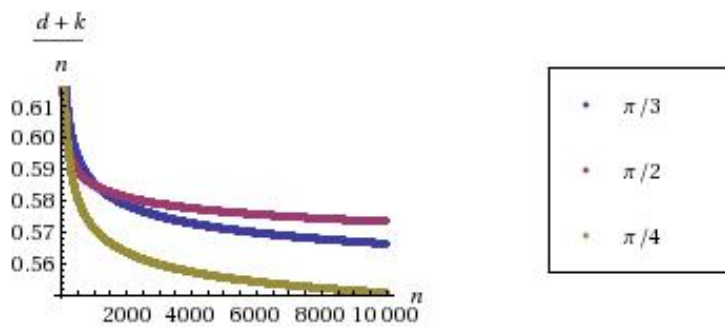


Figure 6: The bound $(k+d)/n$ using $\theta = \pi/3, \pi/4, \pi/2$ when the binary rate $R_2 := 1/2$ and enumerating over the binary block size n . We notice when $n = 10000$, the three curves from top to bottom will be corresponding to $\theta = \pi/2, \pi/3, \pi/4$.

References

- [1] E. Arikan, *Channel polarization: A method for constructing capacity-achieving codes*, Information Theory, 2008. ISIT 2008. IEEE International Symposium on, july 2008, pp. 1173–1177.
- [2] E. Arikan and E. Telatar, *On the rate of channel polarization*, Information Theory, 2009. ISIT 2009. IEEE International Symposium on, 28 2009-july 3 2009, pp. 1493–1495.
- [3] William Feller, *An introduction to probability theory and its applications. Vol. I*, Third edition, John Wiley & Sons Inc., New York, 1968. MR 0228020 (37 #3604)
- [4] G.D. Forney, *Concatenated codes*, M.I.T. research monograph no. 37, Mit Press, 1966.
- [5] Naveen Goela, Emmanuel Abbe, and Michael Gastpar, *Polar codes for broadcast channels*, CoRR **abs/1301.6150** (2013).
- [6] J. P. Hansen and H Stichtenoth, *Group codes on certain algebraic curves with many rational points*, Appl. Algebra Engrg. Comm. Comput. **1** (1990), no. 1, 67–77. MR 1325513 (96e:94023)
- [7] N. Hurt, *Many rational points, coding theory and algebraic geometry*, Kluwer Academic Publishers, Dordrecht, The Netherlands, 2003.
- [8] N. Hussami, R. Urbanke, and S.B. Korada, *Performance of polar codes for channel and source coding*, Information Theory, 2009. ISIT 2009. IEEE International Symposium on, 28 2009-july 3 2009, pp. 1488–1492.
- [9] Wolfram Research Inc, *Mathematica edition: Version 8.0 publisher: Wolfram research, inc*, Third edition, John Wiley & Sons Inc., Champaign, Illinois, 2010.
- [10] S.B. Korada, E. Sasöglu , and R. Urbanke, *Polar codes: Characterization of exponent, bounds, and constructions*, Information Theory, IEEE Transactions on **56** (2010), no. 12, 6253–6264.
- [11] Xudong Ma, *Symbol-index-feedback polar coding schemes for low-complexity devices*, CoRR **abs/1201.1462** (2012).

- [12] Hessam MahdaviFar and Alexander Vardy, *Achieving the secrecy capacity of wiretap channels using polar codes*, CoRR **abs/1007.3568** (2010).
- [13] R. Mori and T. Tanaka, *Channel polarization on q -ary discrete memoryless channels by arbitrary kernels*, Information Theory Proceedings (ISIT), 2010 IEEE International Symposium on, june 2010, pp. 894–898.
- [14] ———, *Non-binary polar codes using reed-solomon codes and algebraic geometry codes*, Information Theory Workshop (ITW), 2010 IEEE, 30 2010-sept. 3 2010, pp. 1–5.
- [15] Ryuhei Mori and Toshiyuki Tanaka, *Source and channel polarization over finite fields and reed-solomon matrix*, CoRR **abs/1211.5264** (2012).
- [16] C. Xing S. Ling, *Coding theory, a first course*, Cambridge, Cambridge, UK, 2004.
- [17] Eren Sasoglu, Emre Telatar, and Erdal Arıkan, *Polarization for arbitrary discrete memoryless channels*, CoRR **abs/0908.0302** (2009).
- [18] H. Stichtenoth, *Algebraic function field and code*, Springer, Berlin, 2009.
- [19] T. Tanaka and R. Mori, *Refined rate of channel polarization*, Information Theory Proceedings (ISIT), 2010 IEEE International Symposium on, june 2010, pp. 889–893.
- [20] Michael Tsfasman, Serge Vlăduț, and Dmitry Nogin, *Algebraic geometric codes: basic notions*, Mathematical Surveys and Monographs, vol. 139, American Mathematical Society, Providence, RI, 2007. MR 2339649 (2009a:94055)